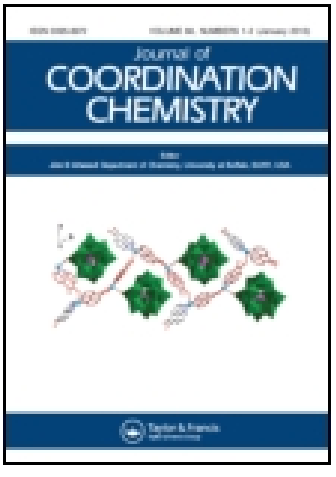

Journal of Coordination Chemistry
Publication details, including instructions for authors and subscription information:
http://www.tandfonline.com/loi/gcoo20

Zeolite-Y enslaved manganese(III) complexes as heterogeneous catalysts

Chetan K. Modi[a] & Parthiv M. Trivedi[b]

[a] Department of Applied Chemistry, Faculty of Technology & Engineering, The Maharaja Sayajirao University of Baroda, Vadodara, India

[b] Department of Chemistry, M.K. Bhavnagar University, Bhavnagar, India

Accepted author version posted online: 07 Oct 2014.Published online: 31 Oct 2014.

To cite this article: Chetan K. Modi & Parthiv M. Trivedi (2014) Zeolite-Y enslaved manganese(III) complexes as heterogeneous catalysts, Journal of Coordination Chemistry, 67:22, 3678-3688, DOI: 10.1080/00958972.2014.973408

To link to this article: http://dx.doi.org/10.1080/00958972.2014.973408

Journal of Coordination Chemistry, 2014
Vol. 67, No. 22, 3678–3688, http://dx.doi.org/10.1080/00958972.2014.973408

Zeolite-Y enslaved manganese(III) complexes as heterogeneous catalysts

CHETAN K. MODI*† and PARTHIV M. TRIVEDI‡[1]

†Department of Applied Chemistry, Faculty of Technology & Engineering, The Maharaja Sayajirao University of Baroda, Vadodara, India
‡Department of Chemistry, M.K. Bhavnagar University, Bhavnagar, India

(*Received 7 January 2014; accepted 17 September 2014*)

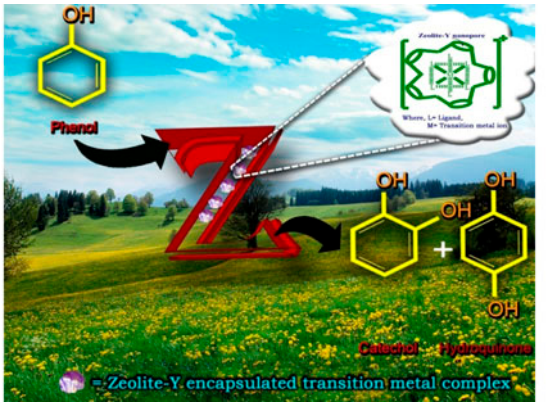

Traditional catalytic procedures for oxidation of phenol produce environmentally undesirable wastes. As a consequence, there is a clear demand for development of an environmentally benign catalytic route for the selective oxidation of phenol. A series of zeolite-Y enslaved Mn(III) complexes with Schiff bases derived from vanillin furoic-2-carboxylic acid hydrazone (VFCH), vanillin thiophene-2-carboxylic acid hydrazone (VTCH), ethylvanillin thiophene-2-carboxylic acid hydrazone (EVTCH), and/or ethylvanillin furoic-2-carboxylic acid hydrazone have been synthesized and characterized by physico-chemical techniques. Catalytic oxidations of phenol using 30% H_2O_2 as an oxidant over $[Mn(VTCH)_2{\cdot}2H_2O]^+$-Y, $[Mn(VFCH)_2{\cdot}2H_2O]^+$-Y, and $[Mn(EVTCH)_2{\cdot}2H_2O]^+$-Y under mild conditions were studied. These zeolite-Y enslaved Mn(III) complexes are stable and recyclable under current reaction conditions.

Keywords: Zeolite-Y; Mn(III) complexes; Liquid-phase oxidation of phenol

*Corresponding author. Email: chetanmodi-appchem@msubaroda.ac.in
[1]Present address: Reliance Industries, Navi Mumbai, India

1. Introduction

Increasingly more restraining policies relating to environmental safety require progress in technology of chemical processes creating interest in catalysis. Molecular sieves have expanded into an imposing group of inorganic-crossbreed materials with huge number of industrial applications, mainly in the field of catalysis. They include zeolites, mesoporous materials, and metal-organic frameworks. In particular, zeolites are crystalline aluminosilicates formed by nanocavities and channels of strictly regular dimensions. In addition, they have drawn attention for potential applications in ion exchange, magnetism, separation, gas storage, nonlinear optics, solar energy conversion, heterogeneous catalysis, etc. [1–7]. The 3-D large internal pore (~13 Å) zeolite-Y has been studied as host lattices. It possesses properties, such as high surface area, crystalline open structures, tunable pore size and functionality, high adsorption capacity, and partitioning of reactant/products, which allows considering them as prospective supports for entrapment of catalytically active complexes [8–10] or metal complexes [11–14]. The as-prepared inorganic-crossbred material not only has heterogeneous catalytic characteristics, but also preserves high catalytic efficiency originating in homogeneous catalysis due to the *site secluded effect*.

One of the major current challenges in synthetic organic chemistry is selective oxidation of organic compounds using 30% H_2O_2 in the presence of transition metal catalysts [15–17]. In particular, oxidation of phenol has been given much attention in industries after the invention of TS-1 and TS-2 catalyzed commercial process using 30% H_2O_2 as an oxidant producing benzenediols [18–20]. Benzenediols viz. catechol (CAT) and hydroquinone (HQ) are important precursors in the production of many valuable products such as pesticides, pharmaceutical product, perfumes, herbicides, and dyestuffs [21, 22].

Manganese is a biologically relevant element and important for health as it helps to absorb or utilize nutrients such as biotin, thiamin, ascorbic acid, and choline (a B-complex vitamin). It is important to know that manganese is an antioxidant and thus fights free radicals and prevents our body from damage caused by free radicals. Studies of manganese compounds derived from various ligands have been developed in recent years, mostly motivated by their intriguing biological features and catalytic applications [23–25]. Manganese complexes encapsulated in the cavity of zeolite-Y have also been reported for oxidation reactions[26–29]. Ratnasamy *et al.* encapsulated metallosalen complexes [Mn^{III}(salen)] in zeolite-X and -Y to study their catalytic activity for oxidation of styrene [30, 31]. Maurya and co-workers studied manganese(III) complexes of pyridoxal-based Schiff base ligands encapsulated in supercages of zeolite-Y. The as-prepared catalysts have been screened for oxidation of phenyl sulfide, styrene, and benzoin [32]. The great applicability of manganese complexes prompted us to prepare manganese(III) complexes enslaved in nanopores of zeolite-Y. These enslaved complexes have been screened for oxidation of phenol using 30% H_2O_2 as oxidant.

2. Experimental

2.1. *Materials*

Analytical reagent grade thiophene-2-carboxylic acid and furoic-2-carboxylic acid from Spectrochem, India; vanillin, phenol, and ethylvanillin from E. Merck, India; and 30% H_2O_2 from Rankem, India were used as obtained. The Schiff base ligands were synthesized

by condensation of vanillin with thiophene-2-carboxylic acid hydrazide and furoic-2-carboxylic acid hydrazide according to reported procedure [33]. $Mn(CH_3COO)_3{\cdot}2H_2O$ was prepared by oxidation of $Mn(CH_3COO)_2{\cdot}4H_2O$ (E. Merck) using Christensen's method [34]. Sodium form of zeolite-Y (Si/Al = 2.60) was procured from Hi-media, India.

2.2. *Instrumentation*

The Si, Al, Na, and Mn(III) ions of the enslaved complexes were determined by ICP-OES (Model: Perkin Elmer Optima 2000 DV). Carbon, hydrogen, and nitrogen were analyzed with a Perkin Elmer, USA 2400-II CHN analyzer. IR spectra of zeolite-Y enslaved Mn(III) complexes were recorded on a Thermo Nicolet IR200 FT-IR spectrometer in KBr. Electronic spectra were recorded on a Varian Cary 500 Shimadzu spectrophotometer. The crystallinity of compounds was ensured by X-ray diffraction (XRD) (Model: Bruker AXS D_8 Advance X-ray powder diffractometer) with a Cu Kα target. The surface areas of the compounds were measured by multipoint BET method using ASAP 2010, micrometrics surface area analyzer. The scanning electron micrographs (SEMs) of enslaved Mn(III) complexes were recorded using a SEM instrument (Model: LEO 1430 VP).

2.3. *Synthesis of Mn(III) based neat complexes*

The procedures for preparation of Mn(III) complexes are 0.02 M vanillin thiophene-2-carboxylic acid hydrazone (VTCH), VFCH, ethylvanillin thiophene-2-carboxylic acid hydrazone (EVTCH), and/or ethylvanillin furoic-2-carboxylic acid hydrazone (EVFCH) ligands were dissolved in 25 mL ethanol and then heated to boiling. This was followed by dropwise addition of a solution of 0.01 M $Mn(CH_3COO)_3{\cdot}2H_2O$ in 10 mL ethanol. The pH of the resulting solution was adjusted to 5–6 by dropwise addition of CH_3COONa solution. The resultant solution was stirred and refluxed for 4 h. After cooling, the solid product was separated by filtration and dried in vacuum.

2.4. *Preparation of Mn(III)-Y (metal exchanged zeolite-Y)*

A series of zeolite-Y enslaved Mn(III)-Y complexes have been prepared by Flexible Ligand Method. 5.0 g of zeolite-Y was suspended in 300 mL of deionized water containing 12 mM $Mn(CH_3COO)_3{\cdot}2H_2O$ with constant stirring. The reaction mixture was then heated at 90 °C for 24 h. The solid was filtered, washed with hot deionized water until the filtrate was free from any metal ion content, and dried for 15 h at 150 °C in air.

2.5. *Preparation of zeolite-Y enslaved Mn(III) complexes*

One gram of metal-exchanged zeolite-Y was uniformly mixed with an excess of ligand ($n_{ligand}/n_{metal} = 3$) in ethanol into a sealed round bottom flask. The reaction mixture was refluxed (~24 h) in an oil bath with stirring. The resulting material was Soxhlet extracted with ethanol, acetone, and finally with acetonitrile (6 h) to remove uncomplexed ligand and the complex adsorbed on the exterior surface of zeolite-Y. The extracted material was ion-exchanged with 0.01 M NaCl aqueous solution for 24 h to remove uncoordinated metal ions, followed by washing with deionized water until no Cl^- ion could be detected with $AgNO_3$ solution. The final product was dried at 120 °C.

Table 1. Catalytic performances over oxidation of phenol to CAT and HQ.

Sr. no.	Compound	Conversion (%)	TOF (h^{-1}) for 6 h	Selectivity (%)	
				Catechol	Hydroquinone
1	Na-Y	3.1	–	44.3	55.7
2	Mn(III)-Y	16.3	–	48.3	51.7
3	$[Mn(VFCH)_2{\cdot}2H_2O]^+$-Y	37.4	75	69.9	30.1
4	$[Mn(VFCH)_2(L)H_2O]$	18.6	–	36.5	63.5
5	$[Mn(VTCH)_2{\cdot}2H_2O]^+$-Y	43.1	85	74.6	25.4
6	$[Mn(VTCH)_2(L)H_2O]$	24.6	–	46.4	53.6
7	$[Mn(EVFCH)_2{\cdot}2H_2O]^+$-Y	19.8	37	52.8	47.2
8	$[Mn(EVFCH)_2(L)H_2O]$	16.5	–	30.7	69.3
9	$[Mn(EVTCH)_2{\cdot}2H_2O]^+$-Y	20.2	38	54.9	45.1
10	$[Mn(EVTCH)_2{\cdot}(L)H_2O]$	17.4	–	39.4	60.6
11	$[Mn(VTCH)_2{\cdot}2H_2O]^+$-Y[a]	41.9	–	72.6	27.4
12	$[Mn(VTCH)_2{\cdot}2H_2O]^+$-Y[b]	39.4	–	69.8	30.2

Note: L = CH_3COO^- ion.
[a]First reused catalyst.
[b]Second reused catalyst.

2.6. *Catalytic oxidation of phenol*

The catalytic oxidation of phenol over zeolite-Y enslaved Mn(III) complexes using 30% H_2O_2 as oxidant were optimized as follows: phenol (30 mM), 45 mM of 30% H_2O_2, catalyst (60 mg), acetonitrile (2 mL) at 80 °C for 6 h. The products were collected at different time intervals and were identified and quantified by GC. Blank experiments were performed over Na-Y, Mn(III)-Y and neat complexes under identical conditions with only negligible conversion (see table 1).

3. Results and discussion

3.1. *Morphological and textural properties of materials*

The results of chemical analyses of neat zeolite-Y and their enslaved Mn(III) complexes are given in table 2, revealing that the Si/Al ratio (i.e. 2.60) is constant even after metal exchange and formation of complexes, confirming the retention of the zeolite framework during complexation. Furthermore, the chemical analyses confirm the presence of Mn(III) complexes in the zeolite matrix. The surface area and pore volume values estimated by nitrogen adsorption isotherms are given in table 3. The results show considerable decrease in the surface area and pore volume of zeolite-Y on entrapment of Mn(III) complexes, confirming the presence of complexes inside the nanopores of zeolite-Y.

Table 2. Analytical data of compounds.

Sr. No.	Compound	Elements %found							
		%C	%H	%N	%M	%Si	%Al	%Na	Si/Al
1	Na-Y	–	–	–	–	17.16	6.60	9.86	2.60
2	Mn(III)-Y	–	–	–	3.69	16.86	6.48	7.73	2.60
3	$[Mn(VFCH)_2{\cdot}2H_2O]^+$-Y	4.65	1.46	0.93	2.29	16.75	6.44	7.11	2.60
4	$[Mn(VTCH)_2{\cdot}2H_2O]^+$-Y	4.79	1.53	0.97	2.33	16.67	6.41	6.90	2.60
5	$[Mn(EVTCH)_2{\cdot}2H_2O]^+$-Y	4.93	1.61	1.02	2.41	16.59	6.38	6.38	2.60
6	$[Mn(EVFCH)_2{\cdot}2H_2O]^+$-Y	4.85	1.57	0.98	2.37	16.70	6.42	7.20	2.60

Table 3. Surface area and pore volume data of Na-Y, Mn(III)-Y and their enslaved complexes.

Compound	Surface area ($m^2\ g^{-1}$)	Pore volume ($cc\ g^{-1}$)[a]
Na-Y	548	0.32
Mn(III)-Y	510	0.27
$[Mn(VFCH)_2{\cdot}2H_2O]^+$-Y	293	0.21
$[Mn(VTCH)_2{\cdot}2H_2O]^+$-Y	219	0.09
$[Mn(EVTCH)_2{\cdot}2H_2O]^+$-Y	291	0.20
$[Mn(EVFCH)_2{\cdot}2H_2O]^+$-Y	271	0.16

[a]Calculated by the BJH-method.

Figure 1 represents SEMs of $[Mn(EVFCH)_2{\cdot}2H_2O]^+$-Y recorded before and after Soxhlet extraction. It is clear from the well-defined crystals after Soxhlet extraction that enslaved Mn(III) complexes have no surface complexes and the particle boundaries on the external surface of zeolite-Y are clearly distinguishable. These micrographs reveal the efficiency of purification procedure to effect complete removal of extraneous complexes, leading to the presence of well-defined entrapment in the nanocavity.

The powder XRD patterns of Na-Y and enslaved Mn(III) complexes recorded at 2θ degree between 2° and 70° are presented in figure 2. The XRD patterns of zeolite-Y enslaved Mn(III) complexes show no appreciable change in peak positions of the diffraction lines of the neat zeolite-Y, indicating that the crystallinity of the zeolitic matrix remained intact upon entrapment of Mn(III) complexes. However, the relative intensities of some of the diffraction lines may undergo slight changes because of entrapment.

3.2. *Spectroscopic characterization*

Table 4 shows a list of FT-IR spectral data of zeolite-Y enslaved Mn(III) complexes. By comparison with VTCH, VFCH, EVTCH, and EVFCH, the IR bands of all the enslaved complexes are weak due to their low contents in the nanocages of zeolite-Y.

The zeolitic bands dominate the FT-IR spectra of the enslaved Mn(III) complexes. However, the presence of characteristic bands of Mn(III) complexes could be distinguished. Mn(III) complexes showed bands at ~3440, ~1620, and ~1280 cm^{-1}, attributable to ν(O–H), ν(C=N), and ν(C–O) stretches of the ligand. The framework vibration bands of zeolite-Y show below 1200 cm^{-1} for all samples. The bands in the 572–584, 718–793, and 1007–1131 cm^{-1} region are attributed to double ring, symmetric stretching, and antisymmetric stretching vibrations, respectively [35]. No shift is observed upon introduction of metal ions and inclusion of metal complexes, further substantiating that the zeolite-Y framework remains unchanged.

Electronic spectral data of Schiff base ligands and their zeolite-Y enslaved Mn(III) complexes are tabulated in table 5. In the exploited wavelength domain from 200 to 900 nm, the Schiff base ligands show an intense band at ~324 nm due to intra-ligand charge transfer transition ($\pi \rightarrow \pi^*$). However, this band undergoes hypsochromic shifts in enslaved Mn(III) complexes resulting from the chelation of the ligand with Mn(III). In particular, the electronic spectra of $[Mn(EVTCH)_2{\cdot}2H_2O]^+$-Y showed a band at 759 nm corresponding to $^5B_{1g} \rightarrow {}^5E_g$ transition [36]. The present Mn(III) complexes are all six coordinate, therefore, either octahedral or distorted octahedral geometry around the metal ion is expected. The appearance of the said band suggests distorted octahedral structures. Such distortion is most probably due to the Jahn–Teller effect as well as the steric effect of the bulky ligands.

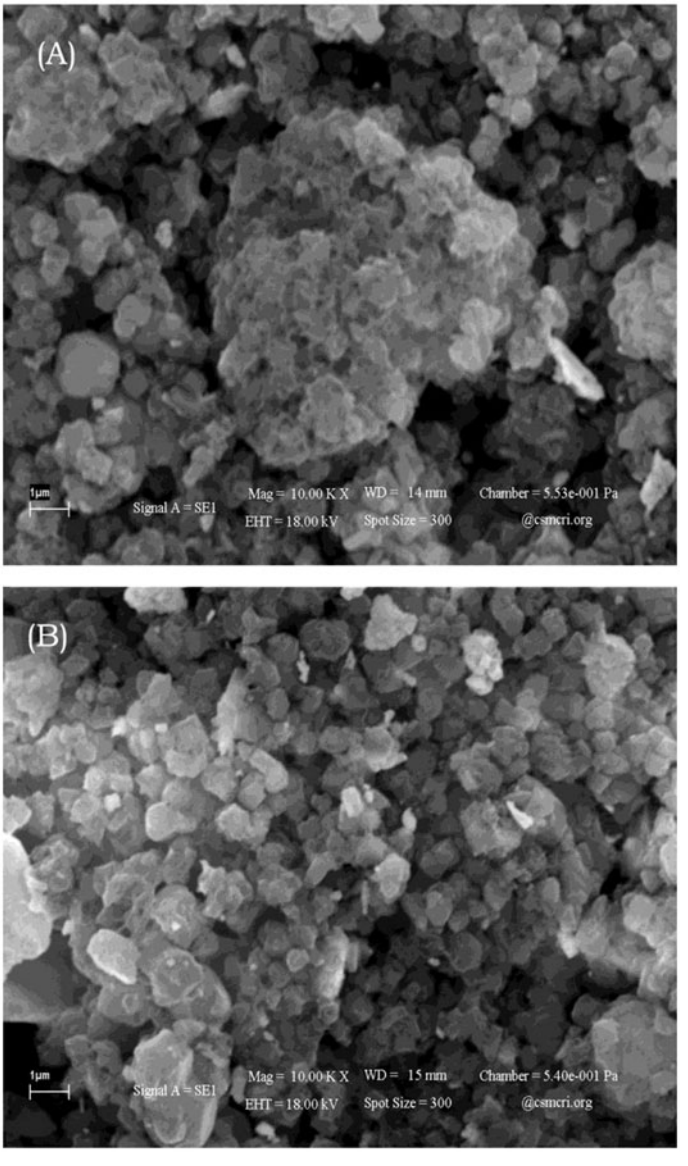

Figure 1. SEM images of $[Mn(EVFCH)_2 \cdot 2H_2O]^+$-Y (A) before and (B) after Soxhlet extraction.

However, we could not observe *d–d* transitions in the remaining Mn(III) enslaved complexes, perhaps due to lower concentration of complex inside the zeolite-Y cavity. Furthermore, the highly intense band observed near 225 nm may be due to MLCT transition.

3.3. *Catalytic activity studies*

The catalytic oxidation of phenol was carried out under optimized reaction conditions. As hydroxyl group on phenol is *ortho* and *para* directing, the oxidation of phenol is expected to give two major products viz. CAT and HQ.

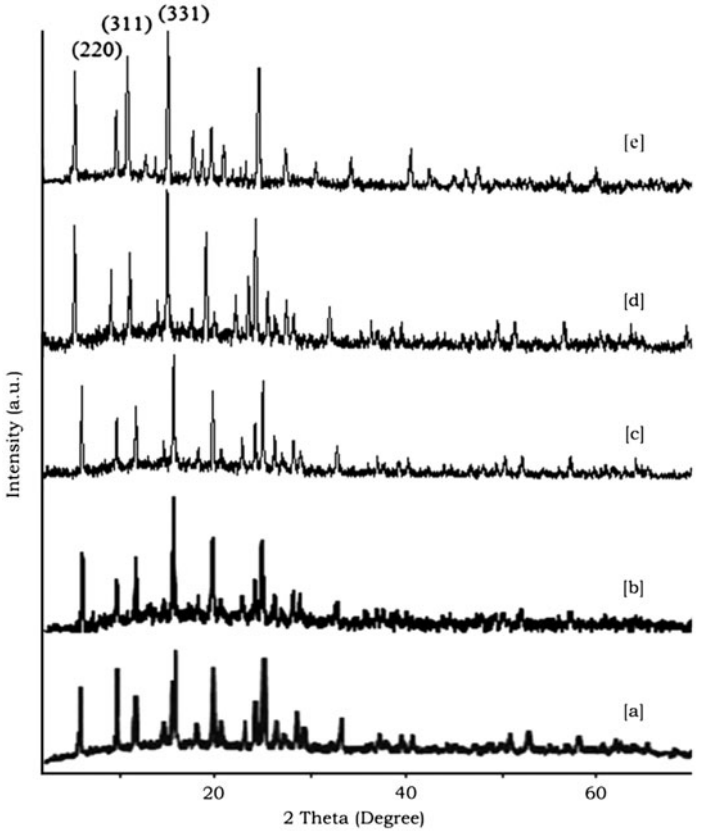

Figure 2. XRD patterns of (a) Na-Y, (b) $[Mn(EVFCH)_2{\cdot}2H_2O]^+$-Y, (c) $[Mn(EVTCH)_2{\cdot}2H_2O]^+$-Y, (d) $[Mn(VFCH)_2{\cdot}2H_2O]^+$-Y, and (e) $[Mn(VTCH)_2{\cdot}2H_2O]^+$-Y.

Table 4. FT-IR assignments of Schiff base ligands with their zeolite-Y enslaved Mn(III) complexes in cm^{-1}.

Compound	Internal vibrations		External vibrations					
	$\nu_{antisym}$T–O	ν_{sym}T–O	ν_{sym}T–O	$\nu_{antisym}$T–O	D–R	$\nu_{(C=N)}$	$\nu_{(O–H)}$	$\nu_{(C–O)}$
VTCH	–	–	–	–	–	1635	3422	1286
VFCH	–	–	–	–	–	1639	3432	1291
EVTCH	–	–	–	–	–	1633	3432	1315
EVFCH	–	–	–	-	–	1626	3430	1312
$[Mn(VFCH)_2{\cdot}2H_2O]^+$-Y	1010	719	785	1118	572	1619	3440	1274
$[Mn(VTCH)_2{\cdot}2H_2O]^+$-Y	1015	718	787	1125	577	1620	3433	1283
$[Mn(EVTCH)_2{\cdot}2H_2O]^+$-Y	1019	724	780	1120	584	1624	3443	1271
$[Mn(EVFCH)_2{\cdot}2H_2O]^+$-Y	1007	720	793	1131	580	1617	3443	1277

3.3.1. Effect of reaction parameters. Figure 3 summarizes the percent conversion of phenol along with CAT and HQ formation. Selectivity of CAT formation varied (44–74%) from catalyst to catalyst. All these catalysts are highly selective toward the CAT formation and the selectivity is maintained even after 24 h reaction time. The effect of amount of catalyst

Table 5. Electronic spectral data of Schiff base ligands with their zeolite-Y enslaved Mn(III) complexes.

Compound	Wavelength (nm)
VTCH	329
VFCH	324
EVTCH	324
EVFCH	346, 205
$[Mn(VFCH)_2{\cdot}2H_2O]^+$-Y	306, 222
$[Mn(VTCH)_2{\cdot}2H_2O]^+$-Y	302, 225
$[Mn(EVTCH)_2{\cdot}2H_2O]^+$-Y	759, 305, 220
$[Mn(EVFCH)_2{\cdot}2H_2O]^+$-Y	303, 249

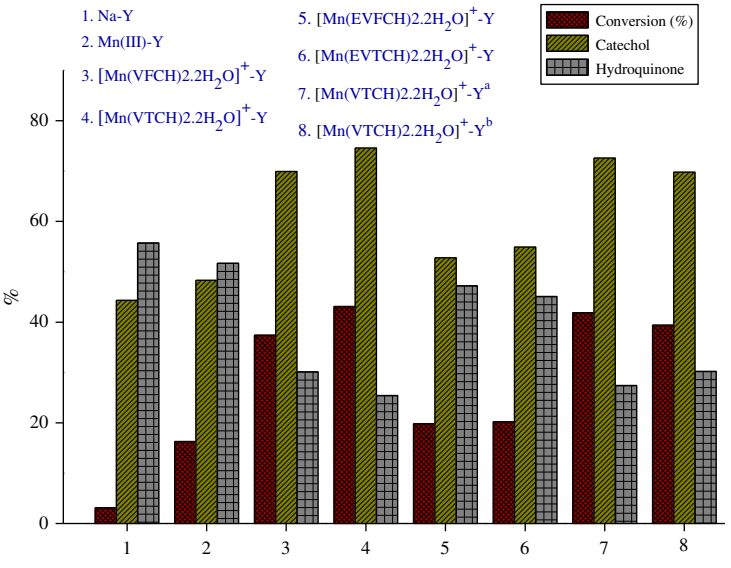

Figure 3. Catalytic conversion (%) of oxidation of phenol (standard deviation = ±0.5%).

and temperature on the oxidation of phenol along with their possible explanations is summarized below:

Influences of the amount of catalysts used for phenol conversion and product selectivity are shown in figure 4. Four different amounts of $[Mn(VTCH)_2{\cdot}2H_2O]^+$-Y as a representative catalyst viz. 40, 50, 60, and 65 mg were used, keeping all other reaction parameters fixed, namely temperature (80 °C), phenol (30 mM), 30% H_2O_2 (45 mM) in acetonitrile (2 mL), and reaction time (6 h). Increase in phenol conversion with increasing catalyst concentration shows that the reaction is catalytic. The conversion (%) decreases beyond 60 mg of catalyst which may be due to fewer catalytic sites and rapid H_2O_2 decomposition was observed at higher catalyst concentration. Therefore, 60 mg of catalyst was taken to be optimal for phenol conversion.

The effect of reaction temperature on phenol conversion is illustrated in figure 5. As expected phenol conversion increased with increasing reaction temperature up to 80 °C and

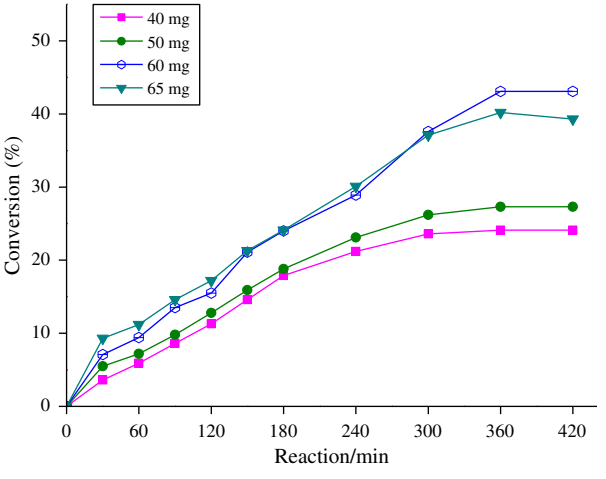

Figure 4. Effect of amount of catalyst on the oxidation of phenol (standard deviation = ±0.5%).

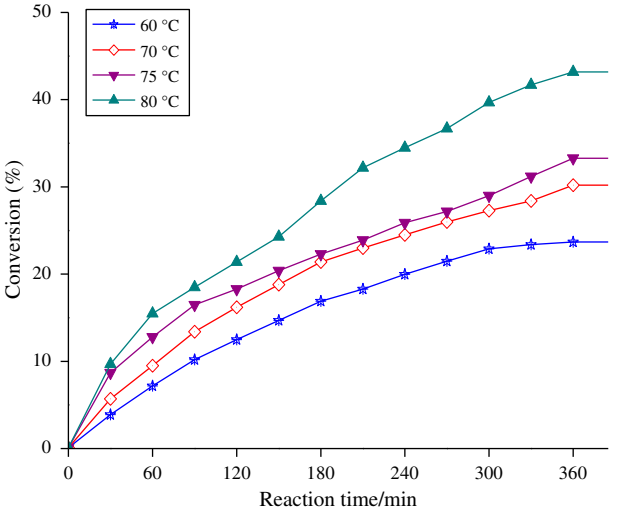

Figure 5. Effect of temperature on the oxidation of phenol (standard deviation = ±0.5%).

higher reaction temperature leads to a dramatic decrease in the selectivity which may be due to rapid decomposition of H_2O_2, as well as significant loss in the conversion. The optimum temperature was 80 °C.

Figure 6 shows that phenol conversion increased with increase in reaction time up to 6 h. An attempt to further increase the phenol conversion by extending the reaction time led to no further conversion; about 90% of H_2O_2 was consumed when the reaction was carried out for 6 h. Decomposition of H_2O_2 is slow initially but increases with time. This indicates that enslaved Mn(III) complex requires longer time to exhibit maximum catalytic activity [37].

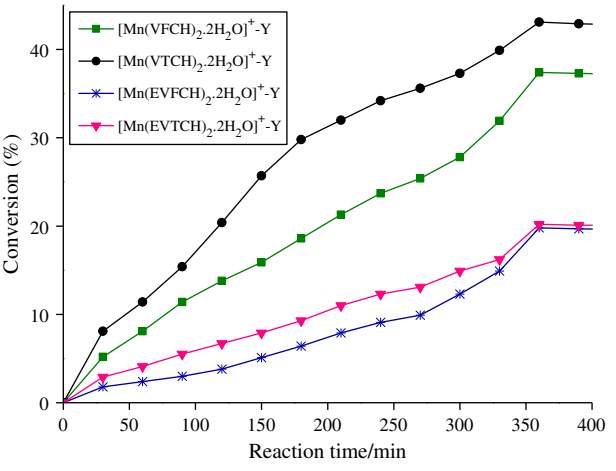

Figure 6. Effect of reaction time on the oxidation of phenol (standard deviation = ±0.5%).

3.3.2. Recyclability of the catalyst. In order to check leaching of metal ions (under optimized reaction conditions), recycling experiment was carried out on the washed catalyst. The representative catalyst $[Mn(VTCH)_2{\cdot}2H_2O]^+$-Y was recycled for oxidation of phenol to establish the effect of encapsulation on stability. The filtrate obtained from $[Mn(VTCH)_2{\cdot}2H_2O]^+$-Y showed further catalytic activity to some extent in the transformation of phenol, indicating slow leaching of metal ions in solution from the cavity of zeolite during reaction. The initial run shows a conversion of 43.1% and it was just marginally reduced to 41.9 and 39.4% after first and second recycling of the catalyst, respectively. These results indicate that $[Mn(VTCH)_2{\cdot}2H_2O]^+$-Y catalyst can be recycled for oxidation of phenol without much loss in activity. Consequently, the encapsulation of metal complexes inside the nanocavity of zeolite-Y increases the life of catalyst by reducing dimerization due to restriction of internal framework structure.

4. Conclusion

- Four manganese(III) complexes were enslaved into the nanopores of zeolite-Y.
- The synthesized heterogeneous nanocatalysts depicted in this article are environmentally benign in liquid phase oxidation of phenol using H_2O_2 as a catalyst.
- Among these enslaved nanocatalysts, $[Mn(VTCH)_2{\cdot}2H_2O]^+$-Y showed the highest catalytic activity (43.1%).

Acknowledgements

We express our gratitude to the Head, Department of Chemistry, M.K. Bhavnagar University, Bhavnagar, Gujarat, India, for providing the necessary laboratory facilities. We also acknowledge the CSMCRI, Bhavnagar, India, for providing the analytical facility.

References

[1] L.V.C. Rees, T. Zuyi. *Zeolites*, **6**, 201 (1986).
[2] A.-K. Boës, B. Xiao, I.L. Megson, R.E. Morris. *Top. Catal.*, **52**, 35 (2009).
[3] M. Miyamoto, Y. Fujioka, K. Yogo. *J. Mater. Chem.*, **22**, 20186 (2012).
[4] H. Sung, T.T. Pham, K.B. Yoon. *Korean Chem. Soc.*, **1**, 32 (2011).
[5] G. Calzaferri, O. Bossart, D. Brühwiler, S. Huber, C. Leiggener, M.K. Van Veen, A.Z. Ruiz. *C.R. Chimie*, **9**, 214 (2006).
[6] A. Corma, H. García. *Chem. Rev.*, **102**, 3837 (2002).
[7] A.H. Ahmed. *J. Mol. Struct.*, **839**, 10 (2007).
[8] N. Zhang, X.-F. Zhou. *J. Mol. Catal. A: Chem.*, **365**, 66 (2012).
[9] A.H. Ahmed, M.S. Thabet. *J. Mol. Struct.*, **1006**, 527 (2011).
[10] M. Salavati-Niasari. *J. Mol. Catal. A: Chem.*, **263**, 247 (2007).
[11] M. Salavati-Niasari. *Inorg. Chim. Acta*, **362**, 2159 (2009).
[12] M. Salavati-Niasari. *Polyhedron*, **28**, 2321 (2009).
[13] P.S. Chittilappilly, N. Sridevi, K.K.M. Yusuff. *J. Mol. Catal. A: Chem.*, **286**, 92 (2008).
[14] R.J. Corrêa, G.C. Salomão, M.H.N. Olsen, L.C. Filho, V. Drago, C. Fernandes, O.A.C. Antunes. *Appl. Catal. A: Gen.*, **336**, 35 (2008).
[15] S.B. Ogunwumi, T. Bein. *Chem. Commun.*, **1997**, 901 (1997).
[16] M.T. Reetz, K. Töllner. *Tetrahedron Lett.*, **36**, 9461 (1995).
[17] C. Bolm, G. Schlingloff, K. Weickhardt. *Angew. Chem. Int. Ed. Engl.*, **33**, 1848 (1994).
[18] B. Notari. In *Studies in Surface Science and Catalysis*, T. Inui, S. Namba, T. Tatsumi (Eds), p. 225, Elsevier, Amsterdam (1991).
[19] J.S. Reddy, S. Sivasanker, P. Ratnasamy. *J. Mol. Catal.*, **71**, 373 (1992).
[20] O.A. Kholdeeva, N.N. Trukhan. *Usp. Khim.*, **75**, 460 (2006).
[21] G. Yang, X. Hu, Y. Wu, C. Liu, Z. Zhang. *Catal. Commun.*, **26**, 132 (2012).
[22] R. Klaewkla, S. Kulprathipanja, P. Rangsunvigit, T. Rirksomboon, W. Rathbun, L. Nemeth. *Chem. Eng. J.*, **129**, 21 (2007).
[23] J.E. Sheats, R.S. Czernuszewicz, G.C. Dismukes, A.L. Rheingold, V. Petrouleas, J. Stubbe, W.H. Armstrong, R.H. Beer, S.J. Lippard. *J. Am. Chem. Soc.*, **109**, 1435 (1987).
[24] F. Bruyneel, C. Letondor, B. Bastürk, A. Gualandi, A. Pordea, H. Stoeckli-Evans, R. Neier. *Adv. Synth. Catal.*, **354**, 428 (2012).
[25] T. Katsuki. *Coord. Chem. Rev.*, **140**, 189 (1995).
[26] S.P. Varkey, C. Ratnasamy, P. Ratnasamy. *J. Mol. Catal. A: Chem.*, **135**, 295 (1998).
[27] M. Salavati-Niasari. *Microporous Mesoporous Mater.*, **95**, 248 (2006).
[28] L.-G. Qiu, A.-J. Xie, L.-D. Zhang. *Adv. Mater.*, **17**, 689 (2005).
[29] I. Kuźniarska-Biernacka, A.M. Fonseca, I.C. Neves. *Inorg. Chim. Acta*, **394**, 591 (2013).
[30] S.P. Verkey, C. Ratnasamy, P. Ratnasamy. *Microporous Mesoporous Mater.*, **22**, 465 (1998).
[31] S.P. Verkey, C.R. Jacob, P. Ratnasamy. *Appl. Catal. A: Gen.*, **182**, 91 (1999).
[32] M.R. Maurya, P. Saini, C. Haldar, F. Avecilla. *Polyhedron*, **31**, 710 (2012).
[33] C.K. Modi, P.M. Trivedi. *J. Coord. Chem.*, **65**, 525 (2012).
[34] O.T. Christensen. *Z. Anorg. Chem.*, **27**, 321 (1901).
[35] A.H. Ahmed, A.G. Mostafa. *Mater. Sci. Eng., C*, **29**, 877 (2009).
[36] I.A. Patel, P. Patel, S. Goldsmith, B.T. Thaker. *Ind. J. Chem., A*, **42**, 2487 (2003).
[37] M.R. Maurya, S.J.J. Titinchi, S. Chand. *J. Mol. Catal. Chem.*, **193**, 165 (2003).